Biomedicine & Pharmacotherapy 192 (2025) 118660

Contents lists available at ScienceDirect

Biomedicine & Pharmacotherapy

journal homepage: www.elsevier.com/locate/biopha

The role of H_2S in isoproterenol-induced cardiac hypertrophy: A comparative study using slow releaser GYY4137 and a newly synthetized fast releaser BM-112

Alexandra Gyöngyösi [a], Simon Eskeif [a,b], Richard Kajtár [a,b], Ferenc Fenyvesi [c], Adina Fésüs [a], Pál Herczegh [d,e], Anikó Borbás [d], Ilona Bereczki [d,e], István Lekli [a,*]

[a] University of Debrecen, Faculty of Pharmacy, Department of Pharmacology, Rex Ferenc utca 1, Debrecen 4002, Hungary
[b] University of Debrecen, Doctoral School of Pharmaceutical Sciences, Egyetem tér 1, Debrecen 4032, Hungary
[c] University of Debrecen, Faculty of Pharmacy, Department of Molecular and Nanopharmaceutical, Rex Ferenc utca 1, Debrecen 4002, Hungary
[d] University of Debrecen, Faculty of Pharmacy, Department of Pharmaceutical Chemistry, Egyetem tér 1, Debrecen 4032, Hungary
[e] HUN-REN-UD Pharmamodul Research Group, University of Debrecen, Egyetem tér 1, Debrecen 4032, Hungary

ARTICLE INFO

Keywords:
Cardiac hypertrophy
Isoproterenol
H_2S
GYY4137
Oxidative stress
Autophagy

ABSTRACT

Cardiac hypertrophy is a compensatory response often associated with cardiovascular diseases. While myocardial hypertrophy provides some advantages at the initial stages of these conditions, sustained hypertrophy can damage the heart, leading to arrhythmia and heart failure. An increasing number of H_2S donors, with diverse chemical and pharmacological properties, have been identified as potential therapeutic agents against oxidative stress and myocardial hypertrophy, with the possibility of regulating autophagy. The aim of this project was to investigate the effect of H_2S on isoproterenol (ISO)-induced cardiac hypertrophy and oxidative stress, as well as its impact on mitochondrial function and autophagy. As exogenous H_2S sources, we employed a newly synthesized fast H_2S-releasing aspirin derivative (BM-112) and GYY4137 a known slow releasing donor. Our results confirmed that H_2S was successfully released from BM-112 in a cell culture medium, and each compound enhanced significantly the intracellular level of H_2S, as measured using the HSip-1 DA probe. Biocompatibility of BM-112 was assessed using MTT assay, which showed no cytotoxic effect on H9c2 at concentrations below 50 μM. Both H_2S releasing molecules, BM-112 and GYY4137, significantly inhibited ISO-induced hypertrophy in cardiomyocytes, as evidenced by decreased cell size. GYY4137 effectively inhibited ISO-induced oxidative stress (DCF-DA) and mitigated mitochondrial dysfunction (MitoSOX Red and JC-1), whereas BM-112 failed to alleviate these effects. Changes in autophagic protein expressions were analyzed by Western blot, and LC3B/p62 colocalization was visualized with Lysotracker Red. We identified impaired autophagic flux in the presence of ISO and BM-112. However, GYY4137 treatment promoted autophagy beyond basal levels.Taken together, GYY4137, but not BM-112, successfully prevented adrenergic overstimulation-induced hypertrophy by reducing oxidative stress, mitigating mitochondrial dysfunction, and enhancing autophagic flux.

1. Introduction

Cardiac hypertrophy, a key contributor to cardiac damage, ischemia, myocardial infarction and heart failure, is a major global cause of morbidity and mortality. It is defined by a persistent increase in the mass of the heart muscle due to stress on the walls during either systole or diastole [1]. This condition commonly arises during normal development, pregnancy, or as a response to prolonged physical exercise and is called physiological cardiac hypertrophy [2]. At the cellular level, cardiac hypertrophy is marked by enlarged cell size in the absence of cell division, increased protein synthesis with reprogramming of gene expression, increased myocardial oxidative stress, impaired protein and mitochondrial quality control, altered sarcomere structure, and insufficient angiogenesis and elevated cell death. Due to the mentioned

* Corresponding author.
E-mail addresses: gyongyosi.alexandra@pharm.unideb.hu (A. Gyöngyösi), eskeif.simon@mailbox.unideb.hu (S. Eskeif), kajtar.richard@pharm.unideb.hu (R. Kajtár), fenyvesi.ferenc@pharm.unideb.hu (F. Fenyvesi), fesus.adina@pharm.unideb.hu (A. Fésüs), herczegh.pal@pharm.unideb.hu (P. Herczegh), borbas.aniko@pharm.unideb.hu (A. Borbás), bereczki.ilona@pharm.unideb.hu (I. Bereczki), lekli.istvan@pharm.unideb.hu (I. Lekli).

https://doi.org/10.1016/j.biopha.2025.118660
Received 12 August 2025; Received in revised form 3 October 2025; Accepted 16 October 2025
Available online 21 October 2025

processes cardiac hypertrophy becomes maladaptive decompensation [3]. Isoproterenol (ISO), a type of catecholamine, is frequently utilized in experimental models to induce hypertrophy, as it mimics extended adrenergic stimulation and acts as a crucial marker for the progression of maladaptive cardiac hypertrophy. Importantly, the structural changes induced by ISO in the heart vary based on the dosage, mode of administration, and duration of treatment [4,5]. Hydrogen sulfide (H_2S) is recognized as the third most significant endogenous gas signaling molecule in the body, following carbon monoxide (CO) and nitric oxide (NO) [6]. It can be endogenously synthesized in cells through the actions of cystathionine gamma-lyase (CSE), cystathionine beta-synthetase (CBS), and/or 3-mercaptopyruvate sulfurtransferase (3-MST). The distribution of H_2S across tissues is not uniform. Initial methods estimated H_2S concentrations in the vasculature to range from 10 to 100 μM, though more recent studies suggest controversial findings, indicating levels might be in the low nanomolar range [7]. However, even a small amount of highly concentrated H_2S can have lethal effects within a short time if inhaled [8].

Research has shown that H_2S is involved in various pathophysiological processes, including oxidative stress, inflammation, apoptosis, and angiogenesis [7,9]. In recent years, accumulating evidence has highlighted H_2S as a key regulator of heart function, with a protective role in the onset and progression of heart diseases. The cardioprotective effects of H_2S are attributed to its antioxidative properties, preservation of mitochondrial function, reduction of cardiomyocyte apoptosis, anti-inflammatory actions, promotion of angiogenesis, regulation of ion channels, and enhancement of NO production [9]. Hyperstimulation of β-adrenergic receptors, known to induce hypertrophy in cardiomyocytes, can significantly decrease endogenous H_2S level [10].

However, the precise mechanisms through which H_2S impacts cardiac hypertrophy remain unclear. Some studies suggest that the effects of H_2S on myocardial hypertrophy vary across different models [11–13]. Thus, it is crucial to investigate the specific mechanisms by which H2S may delay or reverse myocardial hypertrophy.

As a result, an increasing number of H_2S donors with diverse chemical and pharmacological properties have been identified as potential therapeutic agents. Among these, Na2S and NaHS were the first "H_2S-releasing" compounds studied for their effects on the cardiac system. Subsequently, synthetic H_2S-releasing compounds have been developed, including GYY4137, a water-soluble compound that releases H_2S slowly and has been widely studied for its protective effects on cardiac cells [14]. As new H_2S-releasing agents or donors are developed, these compounds should aim to address clinically significant factors such as sustained release or extended half-life, routes of administration, tissue specificity, and minimal toxicity.

The primary objectives of this study were to determine whether exogenous H_2S supplementation can mitigate ISO-induced hypertrophy in H9c2 cells and to explore the role of autophagy in this process. GYY4137, a known H_2S-releaser and BM-112, a new, water soluble, cysteine-activatable, dithioacetate type H_2S-releasing acetylsalicylic acid (aspirin, ASA) derivative, were the focus of this investigation [15]. While aspirin is well-known as an antiplatelet and anti-inflammatory agent that reduces the risk of acute coronary and cerebrovascular events [16], our study prioritized evaluating BM-112. Additionally, we aimed to assess its H_2S-releasing properties, cytocompatibility, and protective effects against ISO-induced hypertrophy, and compare its cellular effects to those of GYY4137.

2. Materials and methods

2.1. Materials

Medium, fetal bovine serum (FBS), MTT, isoproterenol, GYY4137 and chloroquine were sourced from Sigma (St. Louis, MO, USA). JC-1, MitoSOX and Lysotracker were obtained from Life Technologies (Paisley, Scotland). Stain-Free gels and PVDF membrane were supplied by Bio-Rad Laboratories (Hercules, CA, USA). LC3B (#3868), p62 (#5114), Akt (#9272), p-Akt (#4060), CSE (#30068), Nrf2 (#12721) and SOD2 (#13141) antibodies were acquired from Cell Signaling Technology (Boston, MA, USA), CBS antibody (ARP45746_T100) from Aviva Systems Biology, Corp. (San Diego, CA, USA), MPST antibody (AA 1–297) from antibodies-online Inc. (Limerick, PA,USA). For fluorescent microscopy, p62 (ab91526) was purchased from Abcam (Cambridge, UK). BM-112, as a novel, water-soluble H_2S-donor acetylsalicylic acid derivative was designed and synthesized for this study. The schematic representation of BM-112 is shown in Fig. 1.

2.2. Chemical synthesis of BM-112

2.2.1. General information

Acetylsalicylic acid (ASA) and octaethylene glycol were purchased from Merck (Germany). Octaethylene glycol derivatives 1 and 2 and ASA chloride 3 were synthesized according to the literature [17]. TLC was carried out on Kieselgel 60 F254 (Merck, Darmstadt, Germany) with detection by immersing into ammonium molybdate - sulfuric acid solution followed by heating. Flash column chromatography was performed using Silica gel 60 (Merck, Darmstadt, Germany, 0.040–0.063 mm). The ^{1}H-NMR (400 MHz) and ^{13}C-NMR (100 MHz) spectra were recorded by a Bruker DRX-400 spectrometer. Chemical shifts are referenced to Me_4Si (0.00 ppm for ^{1}H) and to the solvent residual signals. MALDI-TOF MS studies were carried out by a Bruker Autoflex Speed mass spectrometer equipped with a time-of-flight (TOF) mass analyzer. In all cases 19 kV (ion source voltage 1) and 16.65 kV (ion source voltage 2) were used. For reflectron mode, 21 kV and 9.55 kV were applied as reflector voltage 1 and 2, respectively. A solid phase laser (355 nm, ≥100 μJ/pulse) operating at 500 Hz was applied to produce laser desorption and 3000 shots were summed. 2,5-Dihydroxybenzoic acid (DHB) was used as matrix and $F_3CCOONa$ as cationising agent in dimethylformamide.

2.2.2. 25-Thioxo-3,6,9,12,15,18,21-heptaoxa-24-thiahexacosyl 2-acetoxybenzoate (acetylsalicylic acid dithioacetyl-octaethyleneglycolyl ester, BM-112)

Octaethylene glycol dithioacetate **2** (444 mg, 1 mmol) was dissolved in dry dichloromethane (10 mL), pyridine (0.8 mL, 10 mmol) was added, the mixture was cooled to 0 °C, and acetylsalicyloyl chloride **3** (500 mg, 2.5 mmol) in 5 mL dry dichloromethane was added dropwise. The mixture was allowed to warm up to room temperature and stirred for 2 days. Saturated $NaHCO_3$ solution (5 mL) was added to the mixture and stirred for 15 min. The mixture was diluted with dichloromethane (50 mL), washed successively with aq. $NaHSO_4$ and water. The organic phase was dried over Na_2SO_4, filtered and evaporated, and the residue was purified by flash column chromatography (hexane-acetone 4:1) to give compound **BM-112** (500 mg, 82 %) as a yellowish solid. $R_f = 0.36$ (hexane-acetone 3:2); ^{1}H NMR (400 MHz, $CDCl_3$): δ (ppm) 8.05 (dd, 1 H, $J = 7.9$, 1.7 Hz, aromatic C*H*), 7.56 (dt, 1 H, $J = 7.8$, 1.7 Hz, aromatic C*H*), 7.31 (dt, 1 H, $J = 7.7$, 1.2 Hz, aromatic C*H*), 7.10 (dd, 1 H, $J = 8.1$, 1.2 Hz, aromatic C*H*), 4.45 – 4.40 (m, 2 H, OCH_2), 3.81 – 3.76 (m, 2 H, OCH_2), 3.73–3.60 (m, 24 H, OCH_2) 3.47 (t, 2 H, $J = 6.3$ Hz, OCH_2), 2.83 (s, 3 H, OCH_3), 2.36 (s, 3 H, SCH_3); ^{13}C NMR (100 MHz, $CDCl_3$): δ (ppm) 169.7, 164.4 (2 C, *C*=O), 133.9, 131.9, 126.0, 123.8 (4 C, aromatic *C*H), 123.2 (1 C, quat.), 70.6, 70.5, 70.4, 69.1, 68.0, 64.2 (15 C, *C*H_2), 39.3 (1 C, *C*H_3), 36.9 (1 C, *C*H_2), 21.0 (1 C, *C*H_3). MALDI-TOF MS: m/z calcd for $C_{27}H_{42}O_{11}Na^+$: 629.2061 $[M+Na]^+$; found: 629.2052.

2.3. Cell culture

The H9c2 cells were sourced from ATCC (CRL-1446, LGC Standards GmbH Wesel, Germany) and cultured in Dulbecco's modified Eagle's medium (DMEM) supplemented with 10 % or 1 % FBS and 1 % penicillin-streptomycin. The cells were maintained at 37 °C in a humidified incubator with 5 % CO_2 and 95 % air. The medium was

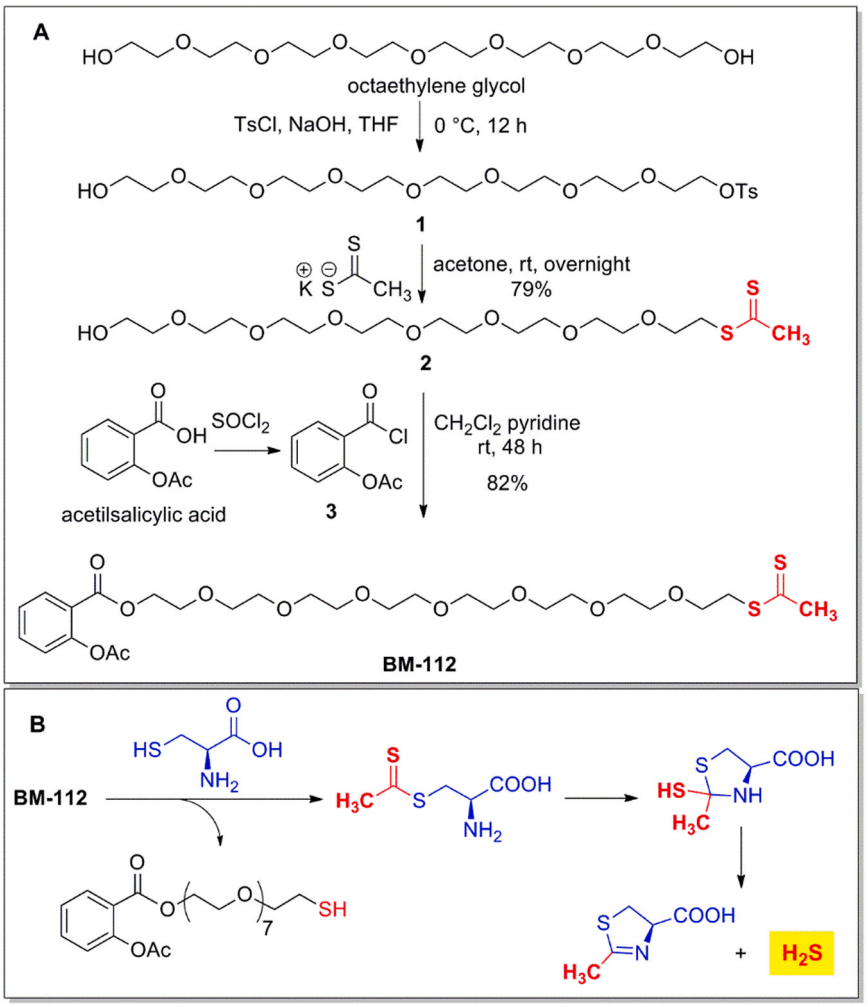

Fig. 1. Synthesis of the new H_2S-releasing derivative of aspirin.

changed every three days, and cells were passaged via trypsinization when they reached 70–80 % confluence. The passage numbers ranged from 8 to 26. Differentiation of H9c2 myoblasts was induced by reducing the serum concentration to 1 % FBS for 18 h [18,19]. Prior to treatment, cells were pre-incubated with 12.5 μM BM-112, ASA, NaHS, or GYY4137, then 30 min later 50 μM ISO was added for 24 h [13]. Fresh stock solutions of all compounds were prepared in the specified medium immediately before use.

2.4. Biocompatibility assessment

For this assay, cells were seeded into 96-well culture plates with 3000 cells/well. Biocompatibility assays were performed by treating the cells with BM-112 at concentrations ranging from 1 to 500 μM in DMEM containing 10 % or 1 % FBS. For combination treatments, 12.5 μM BM-112/ ASA/ NaHS, or GYY4137 was applied, then 30 min later 50 μM ISO was employed. The complete treatment period was 24 h. The protocol was performed as previously described [20]. Results were expressed relative to the control group, which was set as 100 % viability. A 3 % H_2O_2 solution was used as a positive control. Each absorbance value was averaged from eight replicate wells, with experiments repeated 4–6–8 times.

2.5. H_2S-releasing behavior

An amperometric H_2S sensor (ISO-H2S-100) by World Precision Instruments was used to directly measure H_2S levels. The instrument's sensor was connected to a WPI TBR 1025 One-Channel Free Radical Analyzer. H9c2 cells were cultured in DMEM supplemented with either 10 % or 1 % FBS. After three days of incubation, the medium was collected, and BM-112 and GYY4137 were dissolved in the medium to a final concentration of 50 μM and 12.5 μM, respectively. H_2S emissions were monitored continuously over a 24-hour period at ambient temperature. Control experiments were performed without the addition of BM-112 or GYY4137.

2.6. Intracellular H_2S detection by Hsip-1 DA probe

Intracellular H_2S levels were measured using the sensitive fluorescent turn-on probe Hsip-1 DA, which is based on azamacrocyclic copper (II) ion complex chemistry. Upon entering the cells, Hsip-1 DA is hydrolyzed by esterases to form Hsip-1, enabling the selective detection of intracellular H_2S via fluorescence (Excitation: 470–490 nm; Emission: 510–550 nm). It emits strong green fluorescence upon reacting with H_2S. Briefly, cells were seeded in 24-well plates. After cell adhesion, the medium was replaced with 1 % FBS-containing medium for 18 h. The cells were then treated with 12.5 μM BM-112, GYY4137, or NaHS. After 30 min, 50 μM ISO was added and incubated for 1, 2, or 24 h. Subsequently, cells were washed with Hank's Balanced Salt Solution (HBSS). Hsip-1 DA (working concentration: 30 μM) was added for 30 min to allow diffusion into the cells. After incubation, the supernatant was discarded, and the cells were washed with HBSS. The cells were then trypsinized, and fluorescence intensity was measured using a Guava EasyCyte 6HT-2L flow cytometer (Merck Ltd., Darmstadt, Germany).

Fluorescence measurements were analyzed in a time-dependent manner.

2.7. Measurement of the cell surface area

H9c2 cells cultured in 24-well plates were fixed with 4 % paraformaldehyde for 15 min at room temperature. The samples were then permeabilized with 0.1 % Triton™ X-100 in phosphate-buffered saline (PBS) for 15 min. Following this, the cells were incubated with rhodamine conjugated-phalloidin (400x stock solution, Invitrogen, Carlsbad, CA, USA) for 30 min and subsequently washed three times with PBS. Coverslips were mounted using Fluoromount™ Aqueous Mounting Medium (Sigma, St. Louis, MO, USA) after staining with 4', 6-diamidino-2-phenylindole (DAPI, Sigma, St. Louis, MO, USA) The cells were then visualized under a fluorescence microscope. Images were captured using a Zeiss Axio Scope.A1 fluorescent microscope with a 40 × objective lens and analyzed using ZEN v.3.10 Software (Carl Zeiss Microscopy GmbH, München, Germany). Surface areas of cells from 50 randomly selected fields per group were measured using integrated image analysis software. The experiments were repeated three times.

2.8. Confirmation of intracellular reactive oxygen species generation (H_2DCF-DA) and mitochondrial superoxide (MitoSOX) level

At first, cells were seeded in black 96-well plates. After cells adhered, the medium was removed and changed to 1 % FBS content medium for 18 h, then washed with PBS. H_2DCF-DA dye was added for 1 h and diffused into cells. At the end of the incubation period an excess amount of the dye was removed, and fresh medium was added back. After 30 min cells were treated as mentioned above. Then, the medium was removed and washed with PBS. Then the intensity of fluorescent compound was detected by fluorescence spectroscopy (FLUOstar OPTIMA, BMG Labtech) with excitation and emission spectra of 485 nm and 528 nm respectively.

In the other experiment, we measured mitochondrial superoxide level by MitoSOX staining. Cells were seeded into 24-well plates, and cardiomyocytes were treated according to the described previously [20].

2.9. Assessment of mitochondrial membrane potential

Mitochondrial membrane potential (MMP) was evaluated using the fluorescent indicator 5,5',6,6-tetrachloro-1,1'3,3'-tetraethylbenzimidazolocarbo-cyanine iodide (JC-1; from Life Technologies (Paisley, Scotland)). Cardiomyocytes were seeded onto 24-well culture plates with coverslips and treated as described earlier. Following treatment, cells were incubated with 1 mg/mL JC-1 in HBSS at 37 °C for 30 min. After incubation, cells were washed with HBSS and fixed with 4 % methanol-free formaldehyde for 15 min at room temperature. Coverslips were then mounted using Fluoromount™ Aqueous Mounting Medium (Sigma, St. Louis, MO, USA) after staining the nuclei with DAPI (Sigma, St. Louis, MO, USA). Fluorescence images were captured using a Zeiss Axio Scope. A1 fluorescent microscope with 63 × oil immersion objective and analyzed with ZEN v.3.10 Software (Carl Zeiss Microscopy GmbH, München, Germany). Fluorescence intensity from the green and red channels was measured in cells from 50 randomly selected cells per group using integrated image analysis software. A shift from red to green fluorescence, indicating a loss of MMP, was assessed by analyzing multiple merged images.

2.10. Protein isolation

Following treatment, total protein fractions were isolated from the grown H9c2 cells according to the method described in reference [21]. The concentration of the isolated protein was measured using a BCA kit from Thermo Scientific (Rockford, IL, USA).

2.11. Western blot analysis

A 25 μg protein sample was loaded onto a 4–20 % Mini-PROTEAN® TGX Stain-Free™ Protein gel and separated by electrophoresis. Exposure to UV light caused trihalo compounds in the stain-free gel to covalently bind to tryptophan residues in the proteins, allowing total protein quantification. The proteins were then transferred onto PVDF membranes using the Trans-Blot Turbo Transfer System for 30 min. Following the transfer, the membranes were briefly exposed to radiation, and fluorescence signals were captured, with signal intensity correlating to the total protein amount. The membranes were blocked with 5 % non-fat dried milk in Tris-Buffered Saline with Tween 20 (TBST) and incubated overnight at 4 °C with primary antibodies (Akt, p-Akt, CSE, CBS, MPST, Nrf2, SOD2, LC3B, and p62 at a 1:1000 dilution in TBST). After washing with TBST, the membranes were treated with HRP-conjugated secondary antibodies (1:3000 dilutions in TBST, 1.5-hour, room temperature). Enhanced chemiluminescence (ECL) signals were developed using Clarity Western ECL substrate (Bio-Rad Laboratories) and detected with the ChemiDoc Touch imaging system (Bio-Rad Laboratories). The chemiluminescent bands and the total protein intensities for each lane were quantified using Image Lab software (version 5.2.1, Bio-Rad Laboratories). Protein density was directly measured on the membranes, representing the total loaded protein. This normalization method eliminated the need for housekeeping proteins. Normalization factors were calculated by dividing the total stain-free intensity of the reference lane by the stain-free intensity of each lane. Protein expression was assessed as normalized volume, calculated by multiplying the normalization factor by the band intensity (volume) [22].

2.12. Autophagy flux determined by fluorescent microscopy

For the analysis of autophagy flux, we used the Lysotracker Red dye, LC3B, and p62 antibodies. For these experiments, cells were seeded on round glass coverslips placed into 24-well culture plates. The treatment protocol was as mentioned above, and the autophagic process was inhibited by chloroquine (10 mM, 18 h). After treatments, the procedure was carried out as described in the previous study [20]. Images were captured by a Zeiss Axio Scope. A1 fluorescent microscope using the 63 × oil immersion objective lens.

2.13. Statistical analysis

The data were presented as mean ± SEM. Statistical analyses were conducted using GraphPad Prism version 8 from La Jolla, CA, USA. Differences between groups were analyzed using one-way analysis of variance (ANOVA), followed by Tukey's multiple comparison tests. During analysis of Western-blot data, after establishing differences among the mean value of the groups, individual groups were compared by unpaired Student's *t*-test. A significance level of $p < 0.05$ was employed. The symbols *, **, *** and **** indicate statistical significance levels of $p < 0.05$, $p < 0.01$, $p < 0.001$, and $p < 0.0001$, respectively.

3. Results

3.1. Biocompatibility of BM-112

MTT assays were performed to assess biocompatibility and determine the IC_{50} value of BM-112. Cells were treated with BM-112 at concentrations ranging from 1 to 500 μM for 24 h. The control group showed 100 % cell viability. BM-112 treated cells exhibited comparable viability in DMEM containing either 10 % or 1 % FBS. Based on the data in Fig. 2A and 2B, BM-112 demonstrated no cytotoxic effects at concentrations between 1 and 50 μM, with over 70 % of H9c2 cells remaining viable after 24 h of exposure. Further analysis indicated that

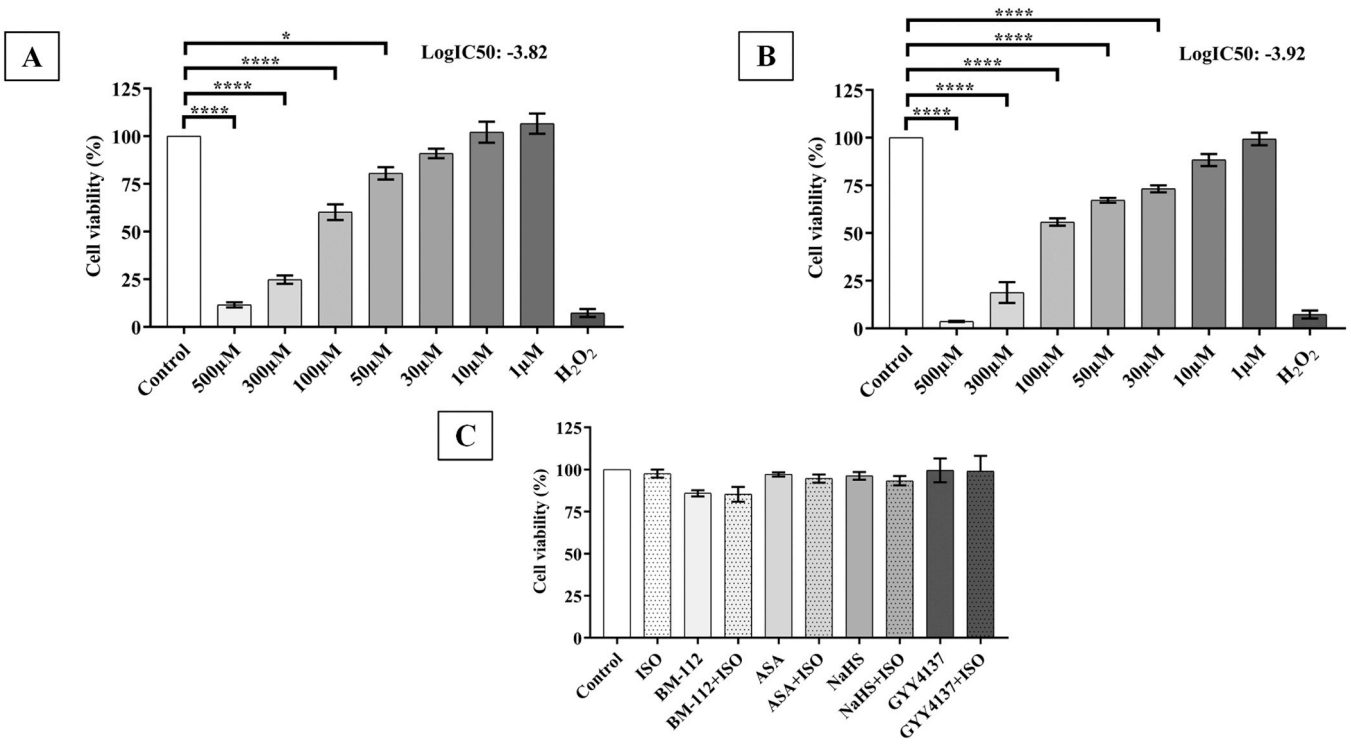

Fig. 2. *Biocompatibility test of BM-112. The H_2S-releasing derivative BM-112 showed no cytotoxic effect on H9c2 at concentrations below 30 μM.* ***(A)*** *H9c2 cells were seeded in DMEM containing 10 % FBS and treated with various concentrations of BM-112 (500–1 h. The logIC_{50} value was determined to be −3.82.* ***(B)*** *H9c2 cells were seeded in DMEM medium with 10 % FBS, then incubated in DMEM containing 1 % h. Subsequently, cells were treated with various concentrations of BM-112 (500–1 h. The logIC_{50} value was determined to be −3.92. h. H9c2 cells were seeded in DMEM medium with 10 % FBS then incubated in DMEM containing 1 % h. min later by 50 μM ISO. Combined treatments showed no significant reduction in cell viability.* Data are expressed as mean ± SEM (n = 4,6,8, respectively). Viability is reported as percentages of cells surviving BM-112 exposure or combined treatment compared to the untreated group. Statistical significance was assessed using one-way ANOVA followed by Tukey's post hoc test. *, and **** represent $p < 0.05$ and $p < 0.0001$, respectively.

using 1 % FBS DMEM, and we did not measure significantly reduced cell viability when cells were treated with 12.5 μM BM-112, ASA, NaHS, or GYY4137 in combination with 50 μM ISO, as shown in Fig. 2C. ASA, NaHS, and GYY4137 served as reference compounds.

3.2. Measurements of H_2S

To measure H_2S liberation, an H_2S sensitive sensor was employed. During the measurements H_2S liberation resulted in an increase in Conductivity (pA). BM-112 or GYY4137 was incubated in a culture medium. Since BM-112 is a new molecule, it was examined at two concentrations (12.5 and 50 μM) in DMEM containing either 1 % or 10 % FBS. The H_2S level began to increase at the start of the experiments and peaked after 16 min, as illustrated in Fig. 3A and B. The amount of H_2S released was only slightly affected by the FBS content of the media (Fig. 3A and B), while, as expected, significantly less H_2S was released from a lower concentration of BM-112. Nevertheless, H_2S was still detectable even at this low concentration. However, GYY4137 released significantly less H_2S, and its presence was hardly detectable with this method (Fig. 3D).

To evaluate the intracellular H_2S levels and verify H_2S release from the compounds, an H_2S-sensitive fluorescent probe was utilized in a time-dependent manner. As shown in Fig. 3E-F, after 1- and 2-hours, BM-112, GYY4137, and NaHS all significantly increased HSip-1 intensity compared to the control indicating an enhanced level of H_2S. As was expected, no difference in intracellular level of H_2S between ISO and control group was found after 1 h. Interestingly, after 24 h incubation with ISO HSip-1staining gave a slightly enhanced intensity. In the case of combined treatment, significant differences were observed only after 24 h (Fig. 3G.). Both BM-112 +ISO and GYY4137 +ISO treatments resulted in a significant increase in fluorescent intensity (Fig. 3H.).

Since endogen H_2S is mainly produced by three enzymes- cystathionine γ-lyase (CSE), cystathionine β-synthase (CBS) and 3-mercaptopyruvate sulfurtransferase (MPST)- we analyzed the expression of these enzymes at the end of the treatments. Interestingly, we measured increased expression of all three enzymes in the ISO-treated group after 24-hour treatment. As depicted in (Fig. 3. I-K) treatment with BM-112 or GYY4137 enhanced the level of CSE.

3.3. H_2S supplementation inhibits ISO-induced myocardial cell hypertrophy

To identify whether H_2S can suppress ISO-induced hypertrophy, cells were treated with ISO in the presence or absence of BM-112 and GYY4137. H9c2 cells were stained with rhodamine-labeled phalloidin and DAPI, then photographed and examined using a fluorescence microscope (Fig. 4A). The cell surface area was measured and analyzed. Our findings revealed a significant increase in the size of H9c2 cells after treatment with ISO, confirming the successful induction of cardiac hypertrophy *in vitro*. Supplemental therapy with the H_2S-releasing compounds BM-112 and GYY4137 significantly prevented cardiomyocytes size enlargement. The cell surface area in the control group was 2558 ± 113 μm², which increased to 3837 ± 152 μm² using 50 μM ISO. Treatment with BM-112 and GYY4137 in the BM-112 +ISO (2920 ± 133 μm²) and GYY4137 +ISO (3151 ± 123 μm²) groups significantly mitigated cell hypertrophy, bringing it closer to the control level (Fig. 4B). To exclude the effect of octaethylene glycol (OCTA), the linker moiety of BM-112, on hypertrophic response, cells were treated with OCTA in the presence or absence of ISO treatment. As shown in S. Fig. 1A-D. OCTA treatment has no influence on cell size, nor on cell viability in the concentration range used. To identify whether H_2S antihypertrophic effect participated in ISO-induced hypertrophy

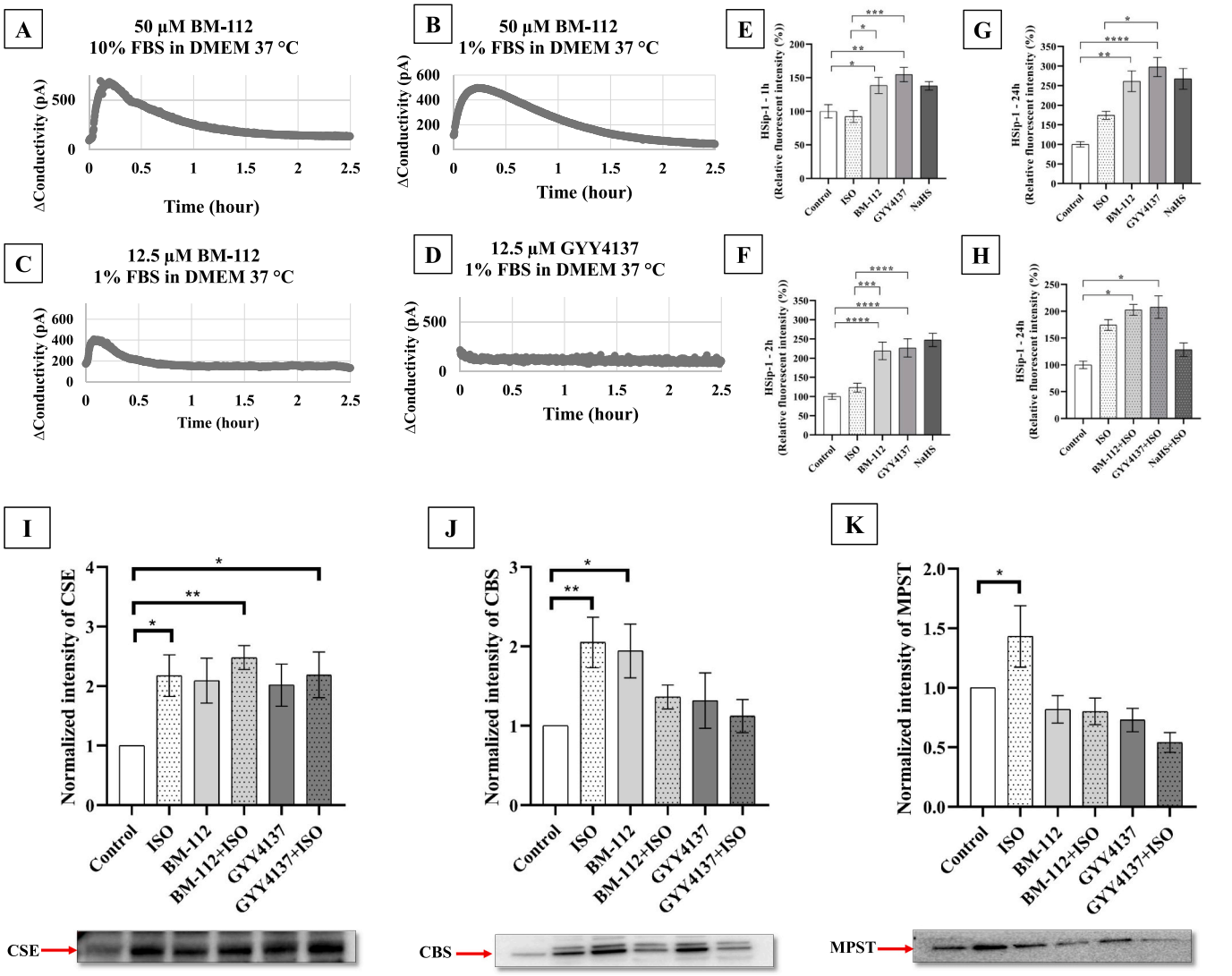

Fig. 3. *H_2S release from BM-112 or GYY4137 and its effects on hypertrophic cardiomyocytes. Changes in extracellular H_2S levels were measured in the culture media after 3 days of incubation with either BM-112 or GYY4137. The influence of exogenous H_2S on the expression of CSE, CBS, and MPST was examined in isoproterenol-induced hypertrophic cardiomyocytes. The treatment conditions were as follows:* ***(A)*** *H_2S release was measured using an H_2S-sensitive sensor in DMEM containing 10 % FBS with 50 µM BM-112.* ***(B)*** 50 µM BM-112 in DMEM containing 1 % FBS. ***(C)*** 12.5 µM BM-112 in DMEM containing 1 % FBS. ***(D)*** *12.5 µM GYY4137 1 % FBS in DMEM.* ***(E-H)*** *Intracellular H_2S were detected using the Hsip-1 DA fluorescent probe as time dependent manner. BM-112, GYY4137, and NaHS were tested at 12.5 µM, with and without 50 µM ISO treatment. Data are presented as mean ± SEM (n = 4).* ***(I-K)*** *Protein expressions of CSE, CBS, and MPST were assessed by Western blotting. Data are presented as mean ± SEM (n = 7, 7 and 4, respectively).* The significance of differences among groups was evaluated with a one-way analysis of variance (ANOVA) followed by Tukey's posttest. *, **, ***, and **** represent $p < 0.05$, $p < 0.01$, $p < 0.001$ and $p < 0.0001$, respectively.

signaling pathway through activation of Akt, western blotting was performed after pretreatment of H_2S-releaser compounds. Our results revealed that under the applied experimental conditions, the ratio of p-Akt/Akt shows no significant changes across groups, thus it has not played a major role (Fig. 4 C). Stimulation of β1-adrenergic receptors rapidly generates ROS as well as impairs the total cellular antioxidant capacity [23]. Thus, the expression of Nrf-2 transcription factor and the enzymatic antioxidant SOD2 protein level were investigated (Fig. 4 D and E). The protein expression of Nrf2 was found to be altered in all the experimental groups, while it was considerably increased in BM-112 and GYY4137 treated cells when compared to that of the control group, while the expression level of SOD2 was significantly increased with GYY4137. Based on our results, we assumed that both H_2S donors could have additional effect on self-defense antioxidant regulation.

3.4. H_2S supplementation by GYY4137 but not BM-112 alleviate ISO-induced oxidative stress

To study the effect of H_2S treatment on intracellular reactive oxygen species (ROS) production in response to ISO treatment, we detected ROS using H_2DCF-DA and mitochondrial superoxide using MitoSOX. H_2DCF-DA can diffuse easily into cells and be oxidized by ROS into 2′, −7′-dichlorofluorescein (DCF). As shown in Fig. 5A, we found an enhanced level of ROS in ISO-treated cells. However, surprisingly, we detected the most intense and significantly higher signal in BM-112 treated cells in the presence (Fig. 5A), or absence (Fig. 5B) of ISO treatment. Interestingly, the slow releasing GYY4137 suppressed ISO-induced ROS formation. This observation led us to perform the experiment in the presence of octaethylene glycol (OCTA), the linker moiety of the compound (S. Fig. 1E-F). Our results indicated that octaethylene glycol enhanced the DCF staining signal, suggesting that this part of the molecule may trigger ROS formation. Next, we examined ROS levels

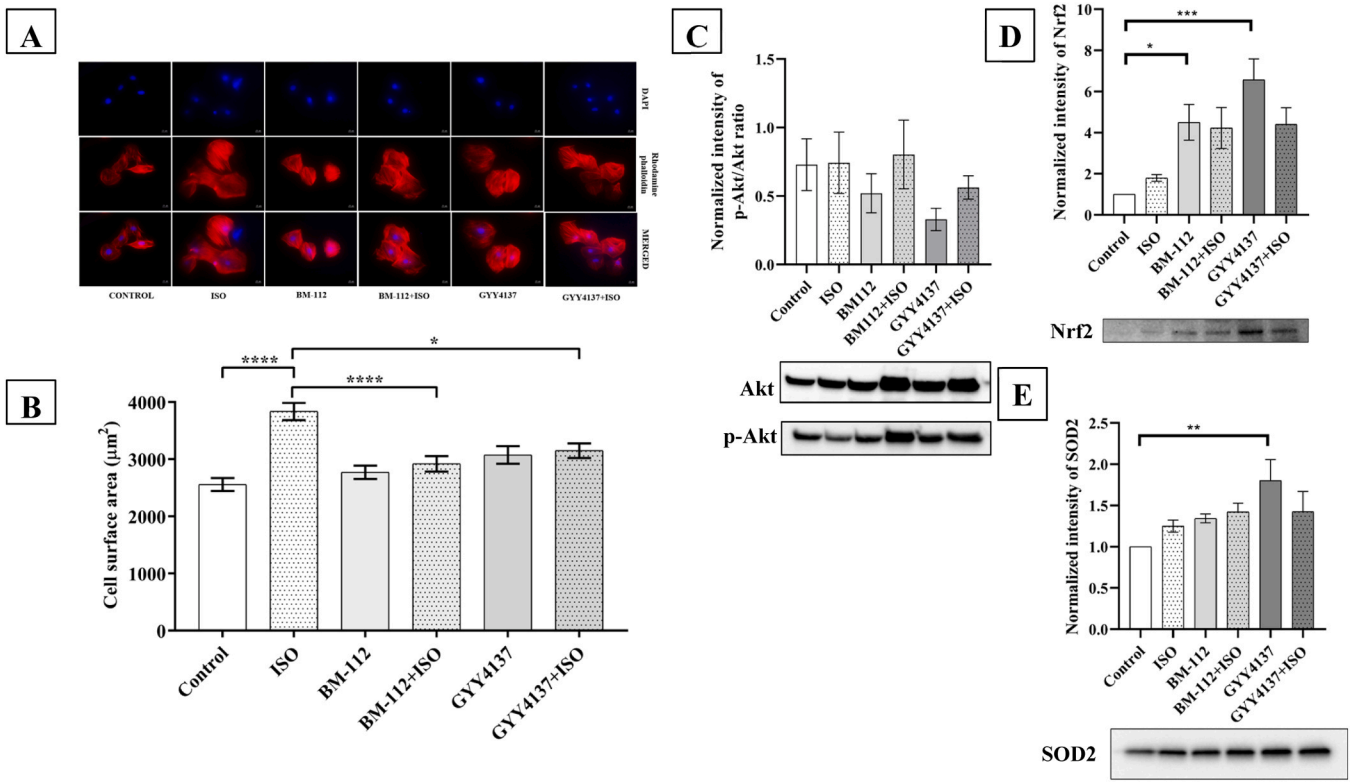

Fig. 4. *H_2S supplementation prevents morphological changes of ISO-induced hypertrophic cardiomyocytes and activates the self-defense pathways against oxidative stress. H9c2 cells were maintained in 1 % serum media for 18 h and treated with 12.5 μM BM-112/12.5 μM GYY4137, and 30 min later with 50 μM ISO for 24 h. The cellular hypertrophy was assayed by rhodamine- labeled phalloidin staining* ***(A)****, then cell surface area was measured* ***(B)****. Images were captured using a Zeiss Axio Scope.A1 fluorescent microscope with a 40 × objective lens and analyzed using* ZEN v.3.10 *Software. Surface areas of cells from 50 randomly selected fields per group were measured using integrated image analysis software. The experiments were repeated three times. Blue channel: DAPI as nucleus staining, Red channel: rhodamine- labeled phalloidin; Merged images. Scale bar represents 20 μm.* ***(C)*** *Western blot analysis of p-Akt/Akt ratio,* ***(D)*** *Nrf2,* ***(E)*** *SOD2* relative protein expressions in H9c2. Values were normalized to the total protein level and expressed as mean ± SEM, n = 7, 7 and 7, respectively. The significance of differences among groups was evaluated with a one-way analysis of variance (ANOVA) followed by Tukey's post test. *, and **** represent $p < 0.05$, and $p < 0.0001$, respectively.

originating from mitochondria. As depicted in Fig. 5 panel C, ISO treatment significantly increased mitochondrial ROS production. BM-112 treatment did not alter ROS levels upon ISO treatment. However, GYY4137, a slow releaser, significantly reduced ROS production in ISO treated cells. These results indicate that the low levels of H_2S supplementation can mitigate mitochondrial ROS formation.

3.5. Impact of H_2S-releasing compound on mitochondrial depolarization of ISO-exposed H9c2 cells

Mitochondria in healthy hearts are relatively abundant and intact, with well-defined membrane structures and clear cristae. However, in hypertrophic hearts, the mitochondria become severely swollen and deformed, with blurred and ruptured membranes and cristae structures [24]. A key feature of dysfunctional mitochondria is a diminished mitochondrial membrane potential (MMP), which is essential for ATP production - a critical process in living cells. In H9c2 cardiomyocytes, JC-1 dye was utilized to evaluate the MMP ($\Delta\psi m$). This dye selectively penetrates mitochondria and undergoes a reversible color change as membrane potential rises (typically above 80–100 mV). In the cytosol, the monomeric form of JC-1 emits green fluorescence, while in healthy mitochondria, its aggregates produce red fluorescence. JC-1 staining was carried out and fluorescent intensity (red/green ratio) was measured to confirm the results. As shown in Fig. 6A, under our experimental condition, we observed a decrease in mitochondrial membrane potential in the ISO-treated group in comparison with control. Surprisingly, in ISO-treated cells supplemented with BM-112, MMP declined even further. In contrast, the slow H_2S-releasing compound GYY4137 restored MMP in ISO-treated cells. This observation led us to investigate the effects of the two H_2S releasers on MMP without ISO treatment. As shown in Fig. 6C, GYY4137 as standalone treatment did not alter MMP; however, BM-112 significantly decreased it. Furthermore, as depicted in S. Fig. 1G-H, OCTA treatment induced mitochondrial depolarization like results observed in BM-112-treated cells.

3.6. Effects of H_2S supplementation on autophagy flux in ISO-induced hypertrophy

To monitor autophagic flux, cells were additionally treated with chloroquine (Q), a well-known autophagic flux inhibitor. Protein expression levels of LC3B-II (Fig. 7A and B) and p62 (Fig. 7C and D) were measured using Western blotting, while lysosome and LC3B or p62 colocalization (Fig. 7E, F, G and H) were visualized by fluorescence microscopy.

An interesting observation was that the presence of H_2S slightly decreased LC3B-II expression, however, there were no significant differences between the groups. As expected, Q treatment significantly increased LC3B-II levels in the treated cells. We have observed a slightly enhanced p62 level in ISO treated cells and significantly decreased p62 in GYY4137 treated cells. As shown in Fig. 7. panels C, D, G, H, chloroquine treatment significantly elevated p62 levels in control cells, indicating basal autophagic flux. However, in ISO-treated cells, after Q treatment p62 levels did not change, suggesting that autophagic flux was impaired. In H_2S supplemented ISO challenged cells Q treatment slightly enhanced p62 expression. Since lysosomes serve as the destination where autophagosomes deliver materials for degradation, Lysotracker

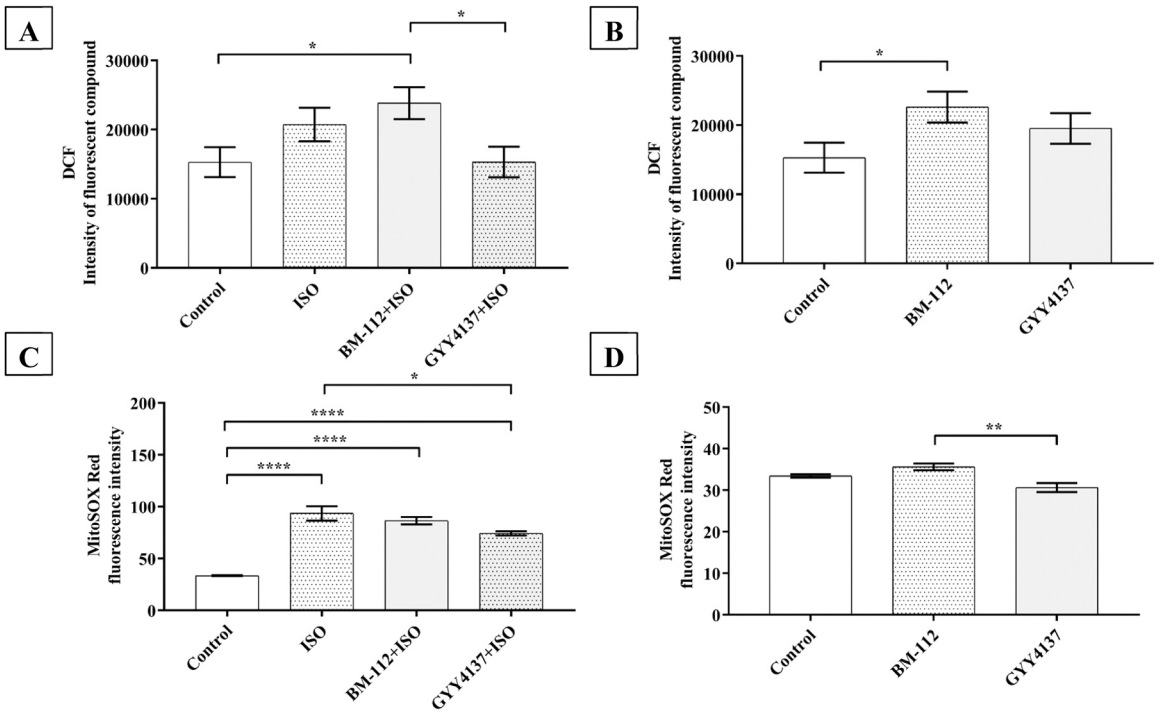

Fig. 5. *Effect of H_2S-releasing compounds on ISO-induced ROS production and mitochondrial superoxide generation in H9c2 cells. Cells were maintained in 1 % serum media for 18 h then treated with 12.5 μM BM-112 or GYY4137 and 30 min later with 50 μM ISO for 24 h. The intracellular ROS and the mitochondrial superoxide levels were estimated using the fluorescent probe H_2DCF-DA* ***(A)*** *and MitoSOX Red* ***(B)*** *respectively, using fluorescence spectroscopy and a flow cytometer. The data summarizes the change in H_2*DCF-DA and MitoSOX Red fluorescence intensity, n = 6 and 4, respectively. The significance of differences among groups was evaluated with a one-way analysis of variance (ANOVA) followed by Tukey's posttest. Data are presented as mean ± SEM, *, ***, and **** represent $p < 0.05$, $p < 0.001$ and $p < 0.0001$, respectively.

Red staining was performed alongside LC3B-II or p62 co-staining. Our immunostaining results with LC3B-II and p62 support the findings obtained from Western blot analysis.

4. Discussion

Hypertrophy, as a key risk factor of cardiovascular disease, is one of the main causes of death in patients suffering from cardiovascular disease worldwide. Despite great progress in elucidating the potential regulatory mechanisms underlying cardiac hypertrophy, there are still some issues to be solved [25]. Studies have indicated that H_2S play an important role in hypertrophy [26]. A reduced total H_2S level was shown in patients suffering from heart failure, a negative relation was found between the plasma level of H_2S and the severity of heart failure [27].

Here we have examined the effects of H_2S supplementation on isoproterenol-induced cardiac hypertrophy. ISO treatment mimics prolonged adrenergic stimulation, which activates different mechanisms in the heart leading to cardiac hypertrophy [28]. We have used GYY4137 and BM-112, our newly synthetized H_2S donor as gasotransmitter. Lee et al. reported that [29] incubation of either NaHS or GYY4137 in culture medium resulted in the release of detectable amounts of H_2S. Release of H_2S from NaHS was rapid peaking at or before 20 min and declining to undetectable levels by 90 min. In contrast, H_2S release from GYY4137 was much lower (<10 % of that observed with NaHS) but was sustained, remaining higher than baseline for up to 7 days. In the current experiments, BM-112 exhibited similar H_2S-releasing kinetics to NaHS, thus it is considered as a fast releaser (Fig. 3).

As expected, the H_2S-releasing molecules significantly enhanced the level of intracellular H_2S. However, a 24-h treatment with ISO also slightly elevated intracellular H2S levels. Endogenous H_2S is generated via 3 enzymes including CSE, CBS, and MPST. ISO treatment significantly upregulated the expression of all three enzymes after 24 h, which may indicate that the cells are enhancing endogenous H_2S production as a protective response to hypertrophic stimuli. Our findings are consistent with those of Geng and colleagues [30], who previously reported increased CSE mRNA expression following ISO treatment, accompanied by decreased H_2S levels. Moreover, exogenous H_2S administration effectively prevented the harmful effects of ISO. CSE and CBS expression levels were slightly increased following H_2S donor supplementation. In agreement with the literature, MPST typically shows no significant change, suggesting that the physiological effects of supplemental H_2S are primarily mediated through CSE and, to a lesser extent, CBS, rather than MPST [31]. However, exogenous H_2S administration at the beginning of the stress, might counteract the hypertrophic effects of angiotensin II (Ang II) and/or noradrenaline (NA) [32] Based on both current and previous results, it appears that under excessive hypertrophic stimulation, cells attempt to upregulate the expression of enzymes involved in endogenous H_2S production; however, this response may be insufficient or delayed for the longer durations.

Our results indicate that BM-112 exhibits no significant cytotoxicity in applied concentration. We have shown that regardless of the kinetics of H_2S release, both molecules significantly enhanced the intracellular H_2S level, and successfully decreased the cell size, thus, reducing ISO-induced hypertrophic response. Earlier, GYY4137 was shown to decrease angiotensin-II-induced cardiac fibroblast proliferation and hypertension-induced myocardial fibrosis [33].

The role of oxidative stress in different cardiovascular disorders including cardiac hypertrophy is well described. Previous studies found that H_2S reduced the ROS generation and accumulation in the myocardium after myocardial ischemia reperfusion [34]. Zhang et al. confirmed that NaHS decreased MDA level and attenuated superoxide anion production, which verified the antioxidative ability of NaHS in myocardium hypertrophy [11]. H_2S supplied by NaHS administration has been shown to upregulate endogen antioxidant proteins downstream to Nrf2 [35]. Consistent with previous studies, our Western blot results showed an increased Nrf-2 protein level following treatment with H_2S donors, which could play at least partially a role in the protective

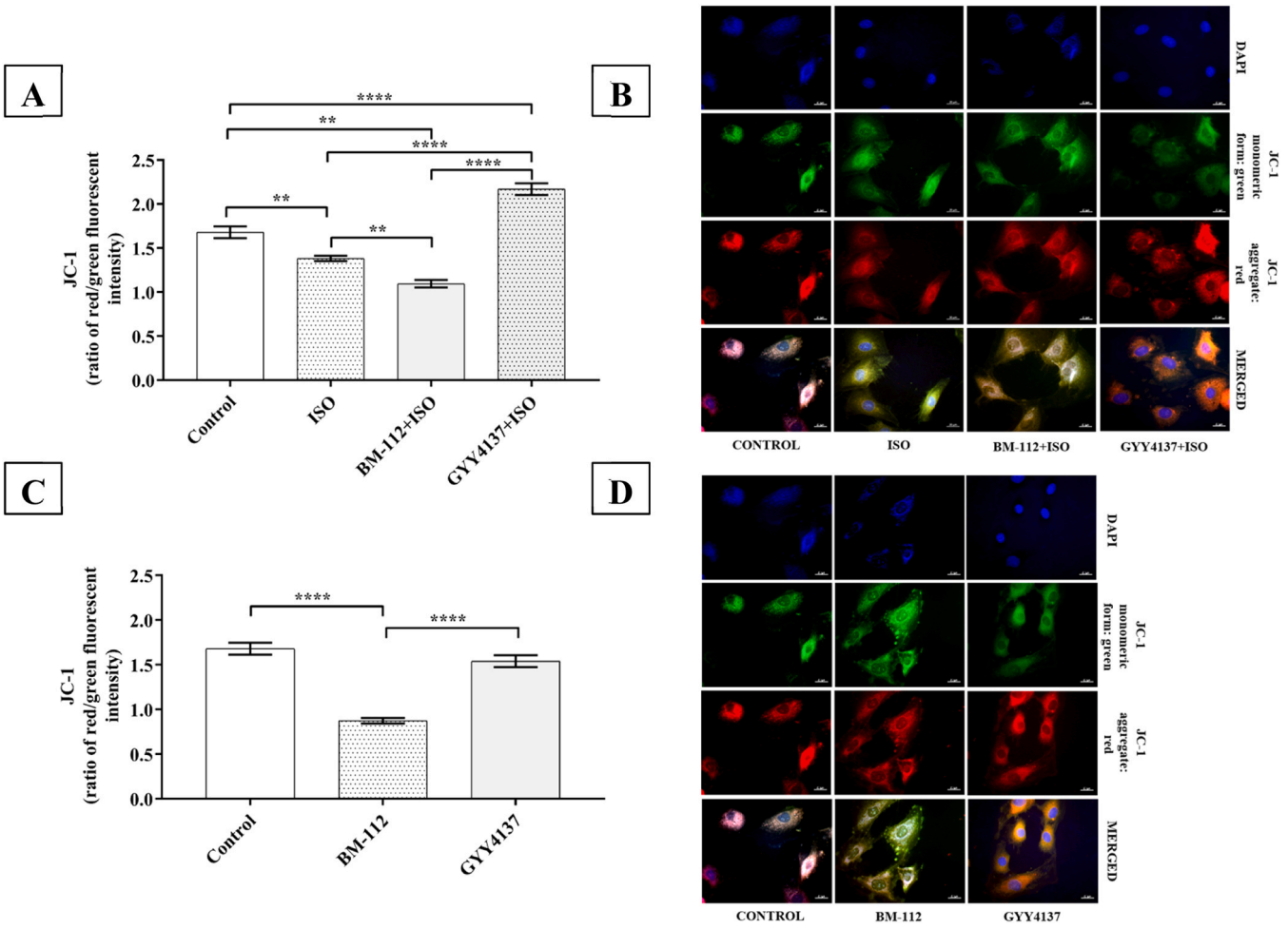

Fig. 6. *Effect of H_2S-releasing compounds on ISO-induced hypertrophy caused mitochondrial membrane depolarization in H9c2 cells. Cells were maintained in 1 % serum media for 18 h and treated with 12.5 μM BM-112 or GYY4137 and 30 min later with 50 μM ISO for 24 h. Then, cells were stained with JC-1, a membrane potential-sensitive fluorescent dye.* ***(A, C)*** Data are presented as mean ± SEM as ratio of red/green fluorescence intensity. n = 60–100 cells/ group. Data are presented as mean ± SEM, *, ***, and **** represent $p < 0.05$, $p < 0.001$, and $p < 0.0001$, respectively. (B and D) Representative images of JC-1 staining. Blue channel: DAPI as nucleus staining, Green channel: JC-1 monomeric form; Red channel: JC-1 aggregated form; Merged images. Scale bar represents 20 μm. Images were captured using a Zeiss Axio Scope.A1 fluorescent microscope with a 63 × oil immersion objective lens and analyzed using ZEN v.3.10 Software.

effects. Interestingly, GYY4137 treatment but nor BM-112 enhanced the expression of SOD2. In line with the above-mentioned literature, our H_2DCF-DA staining indicated enhanced level of ROS in response to ISO treatment, which was decreased by GYY4137 treatment. However, BM-112 enhanced the level of ROS production in the presence or absence of ISO treatment. To explore this phenomenon, we have treated the cells with octaethylene glycol (OCTA), the linker moiety of the molecule. We have found that similarly to BM-112 octaethylene glycol, without ISO-treatment enhanced the ROS formation. Earlier, enhanced mitochondrial ROS production was found in response to ISO-treatment [36], and has been connected to chronic adrenergic stimulation and mitochondrial dysfunction, subsequently linked to progression of heart function decrement [37,38]. Mitochondrial ROS production was studied by MitoSOX Red probe. In line with the literature, we have found enhanced mitochondrial ROS production in ISO-treated cells, which was suppressed by GYY4137 but not BM-112. Consistent with the MitoSOX results, we have detected perturbed mitochondrial membrane potential in ISO challenged cells, which was restored by H_2S liberated from GYY4137. Interestingly, BM-112 decreased mitochondrial membrane potential regardless of ISO administration. On one hand it may be explained by the supraphysiological H_2S level suddenly released from BM-112. The quick release of H_2S may interfere with the cytochrome C oxidase as has been suggested [39,40]. On the other hand, our results with OCTA moiety gave similar results including decreased mitochondrial membrane potential. Thus, it may also contribute to the altered mitochondrial function.

Shao et al. suggested [41] that NaHS exerts a protective effect against myocardial hypertrophy in mice through a PI3K- and/or Akt-dependent pathway. Therefore, we investigated the effect of the H_2S releaser on the phosphorylation of Akt protein. Surprisingly, we observed no significant differences in activation of Akt protein, following treatment with BM-112 and GYY4137 at a concentration of 12.5 μM (Fig. 4. C), which might be explained by different experimental conditions.

Autophagy is an evolutionarily conserved process that degrades and recycles defective organelles, toxic proteins, and various other aggregates on the cytoplasmic surface by sequestering them into autophagosomes which, then, fuse with lysosomes which degrade them [42]. Autophagy plays dual roles in cardiovascular diseases through adaptive or maladaptive regulation [43]. The role of autophagy in isoproterenol-induced cardiomyopathy is still poorly understood [44]. Earlier, we found enhanced LC3B-II expression in ISO-treated animals in a dose-dependent manner, however, in higher doses autophagy was inhibited [5]. On the other hand, pharmacological induction of autophagy in ISO-treated TRL4 KO animals increased cardiac fibrosis [45]. In addition, there has been some controversy on the role of H_2S in autophagy regulation. Recently, an increasing amount of evidence suggests

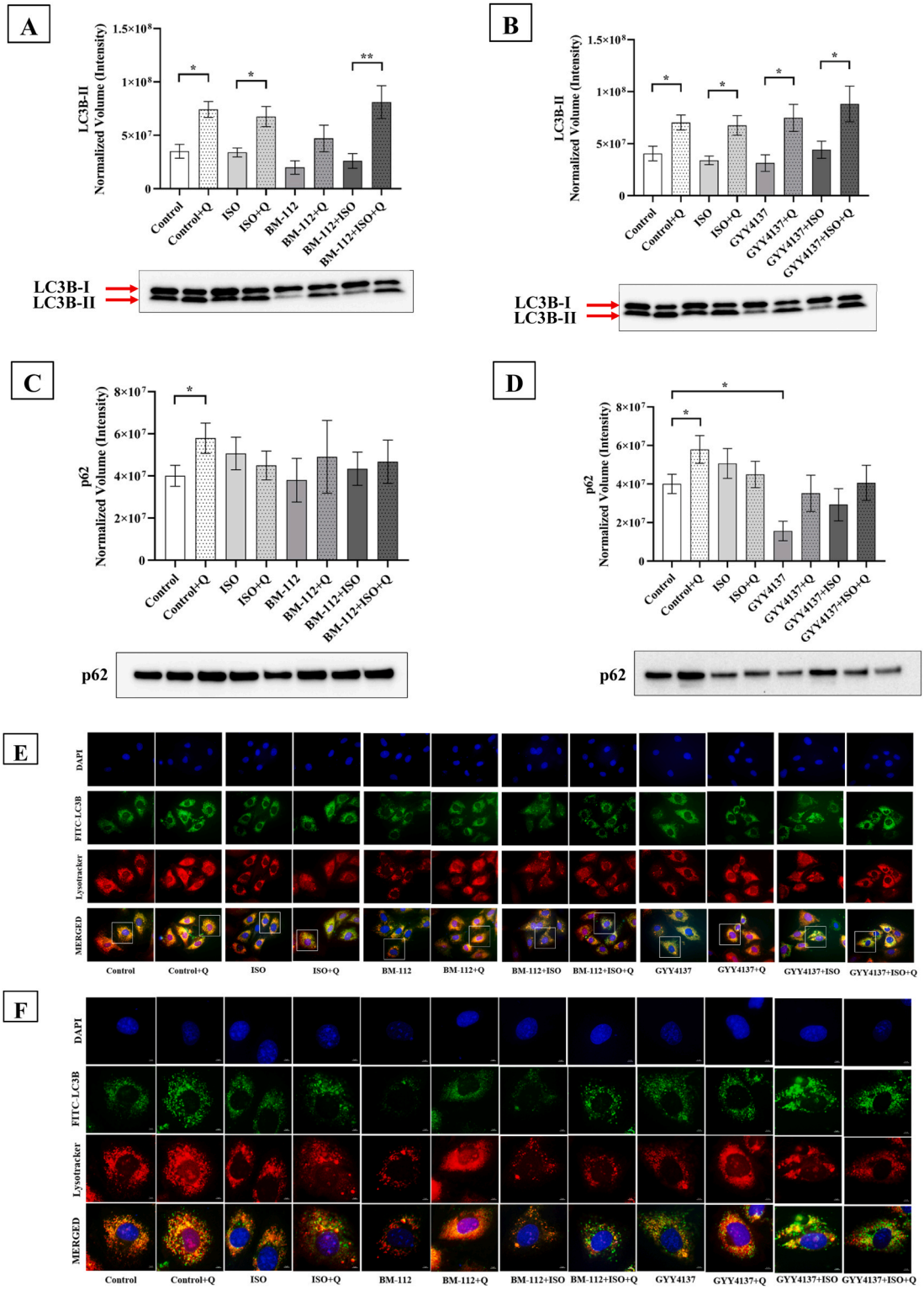

Fig. 7. *Effect of H_2S-releasing compounds and ISO-induced hypertrophy on autophagy flux. Analysis of protein level of LC3B-II* ***(A, B)*** *and p62* ***(C, D)*** *by Western blot. Cells were maintained in 1 % serum media for 18 h and treated with 12.5 μM BM-112 or GYY4137 and 30 min later with 50 μM ISO for 24 h. The autophagic process was inhibited by chloroquine (10 mM, for 18 h).* Values were normalized to the total protein level and expressed as mean ± SEM, n = 14 and 6, respectively. The significance of differences among groups was evaluated with a one-way analysis of variance (ANOVA) followed by Tukey's posttest and Student's *t*-test. * and ** represent $p < 0.05$ and $p < 0.01$. Red arrows indicate the bands for LC3B-I and LC3B-II. Autophagy flux determined by fluorescent microscopy of LC3B **(E, F)** or p62 immunostaining (**G, H**). Representative images show the following: Blue channel: DAPI as nucleus staining; Red channel: Lysotracker Red; Green channel: LC3B or p62 immunostaining; Merged images. Scale bar represents 20 μm (E, G) and 5 μm (F, H). Images were captured using a Zeiss Axio Scope.A1 fluorescent microscope with a 63 × oil immersion objective lens and analyzed using ZEN v.3.10 Software. Quantitative measurements of fluorescence intensity of FITC labeled LC3B (I), p62 (J) and rhodamine labeled lysosomes (K).

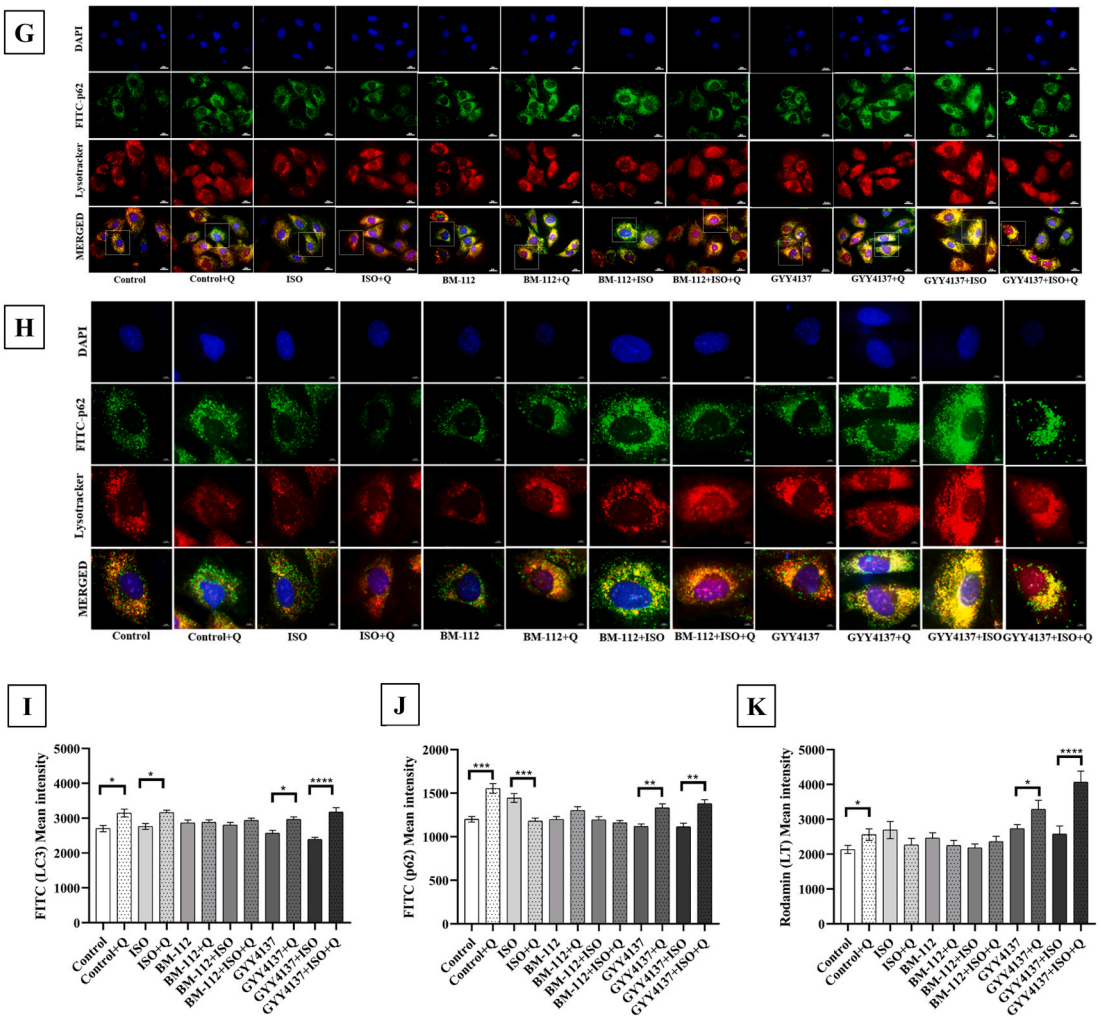

Fig. 7. (*continued*).

that endogenously produced and/or exogenously administered H_2S can exhibit two distinctly opposite effects on autophagy in various disease models. These effects may be attributed to the concentration, time frame, and reaction time of H_2S, as well as differences between disease stages and models [46]. Recent studies indicate that the number of signaling pathways are involved in both pro-autophagy effect and anti-autophagy effect of H_2S, such as PI3K/Akt/mTOR and AMPK/mTOR as called switch phenomena of signaling pathways [46]. In the current study, Western blot analysis showed that LC3B-II and p62 levels have not been changed significantly during treatments, except in ISO and H_2S-treated cells. When chloroquine was applied, the values remained like those of control, except in GYY4137-treated cells. Consistent with the literature, in the ISO-treated groups, LC3B-II levels were not affected by chloroquine treatment, whereas p62 levels were slightly reduced, indicating impaired autophagic flux. Ott and colleagues previously demonstrated that hypertrophic stimuli reduce autophagy, contributing to decreased cardiomyocyte contractility [47]. Furthermore, Wu and colleagues provided exogenous H_2S increased Keap-1 expression by suppressing its ubiquitylation, which might have an important role in ubiquitin aggregate clearance via autophagy, and they presumed autophagy is responsible for the antioxidative effects of H_2S in the context of T2DCM [48]. This observation supports our findings since GYY4137 restored autophagy and suppressed ISO induced oxidative stress. However, in the BM-112-treated group, we observed a slight decrease in LC3B-II levels compared to the control. Additional chloroquine treatment confirmed that autophagic flux was impaired by the newly synthesized compound but not by GYY4137. Following GYY4137 treatment, p62 levels significantly decreased, suggesting that the slow-release H_2S compound promoted autophagy beyond basal levels. In line with our findings, Zhu and colleagues have reported [49] low basal autophagy levels in HUVECs and demonstrated that GYY4137-induced H_2S enhances autophagy in a time- and concentration-dependent manner. Thus, autophagy activated by H_2S exerts vascular-protective actions by activating the Sirt1-FoxO1 signaling pathway, which may be a new mechanism of the anti-atherogenic action of H_2S. Furthermore, using Lysotracker Red, a fluorescent dye that labels acidic organelles, we observed that H_2S-releasing compounds influenced the number of lysosomal puncta. Our microscopic analysis (Fig. 7, panels I–K) showed that GYY4137, but not BM-112, enhanced lysosome numbers, which may be supported by Zhu's results [49]. Based on our Western blot results and microscopic observations, we propose that GYY4137 exerts protective effects against ISO-induced oxidative stress and mitochondrial dysfunction by promoting both autophagosome formation and autolysosome degradation. In contrast, the less effective protective effect of BM-112 may be related to impaired autophagy. Since our results indicate elevated oxidative stress and mitochondrial damage in BM-112 treated groups, we propose that impaired autophagy could either be a cause or a consequence of these effects. Given that the autophagy clearance of damaged or unnecessary mitochondria in cardiomyocytes is delicately regulated by a mitochondria-specific form of autophagy, any disruption in this process may exacerbate cellular dysfunction. Since we have observed reduced

hypertrophy in the presence of both H_2S releasers, with differences in cellular action, we cannot rule out that other mechanisms also play a role in the antihypertrophic effect of H_2S.

In conclusion, H_2S supplementation suppresses ISO-induced hypertrophy by reducing ROS formation and autophagy regulation.

5. Limitation

We successfully demonstrated that both H_2S releasers enhance intracellular H_2S levels. GYY4137 administration resulted in a continuous, low-level release of H_2S over an extended period, allowing for gradual cellular uptake. In contrast, BM-112 released a burst of H_2S, leading to rapid intracellular enrichment. Previous studies have shown that chronic administration of low-dose aspirin (ASA) can suppress hypertrophy. However, in our study, we have not evaluated the effects of ASA under our experimental conditions, making it impossible to rule out its potential contribution to the antihypertrophic effects of BM-112. Additionally, we used octaethylene glycol to study the linker moiety of the molecule. During the chemical synthesis of BM-112, this molecule is incorporated; however, in vivo, following BM-112 metabolism, 1-thiol-octaethylene glycol remains as a metabolite. Further studies are needed to understand its potential biological effects.

CRediT authorship contribution statement

Lekli Istvan: Writing – review & editing, Writing – original draft, Supervision, Resources, Methodology, Funding acquisition, Formal analysis, Conceptualization. **Alexandra Gyöngyösi:** Writing – review & editing, Writing – original draft, Visualization, Project administration, Methodology, Investigation, Formal analysis. **Pál Herczegh:** Writing – review & editing, Conceptualization. **Adina Fésüs:** Methodology, Investigation. **Ilona Bereczki:** Writing – original draft, Methodology, Investigation. **Anikó Borbás:** Writing – review & editing, Writing – original draft, Supervision, Resources, Conceptualization. **Simon Eskeif:** Visualization, Investigation. **Ferenc Fenyvesi:** Methodology. **Richard Kajtár:** Visualization, Investigation.

Consent for publication

Not applicable.

Funding

This work was supported by grants from NKFI-143360 - “Investigation of the effect of biologically active molecules in the cardiovascular system”. Supported by the University of Debrecen Program for Scientific Publication. Project no. TKP2021-EGA-18 has been implemented with the support provided by the Ministry of Culture and Innovation of Hungary from the National Research, Development and Innovation Fund. The project was supported by project no. 2022-1.2.2-TÉT-IPARI-UZ-2022-00006 “Common research and development of different prototypes containing natural herb extract for industrial utilization”.

Declaration of Competing Interest

The authors declare that they have no known competing financial interests or personal relationships that could have appeared to influence the work reported in this paper.

Acknowledgements

The authors thank Márta Bodza for her valuable technical assistance in the synthesis of BM-112.

Appendix A. Supporting information

Supplementary data associated with this article can be found in the online version at doi:10.1016/j.biopha.2025.118660.

Data availability

Data will be made available on request.

References

[1] B.H. Lorell, B.A. Carabello, Left ventricular hypertrophy: pathogenesis, detection, and prognosis, Circulation 102 (4) (2000) 470–479, https://doi.org/10.1161/01.cir.102.4.470.
[2] F. Bazgir, et al., The microenvironment of the pathogenesis of cardiac hypertrophy, Cells 12 (13) (2023), https://doi.org/10.3390/cells12131780.
[3] Y.K. Tham, et al., Pathophysiology of cardiac hypertrophy and heart failure: signaling pathways and novel therapeutic targets, Arch. Toxicol. 89 (9) (2015) 1401–1438, https://doi.org/10.1007/s00204-015-1477-x.
[4] Z. Nichtova, et al., Morphological and functional characteristics of models of experimental myocardial injury induced by isoproterenol, Gen. Physiol. Biophys. 31 (2) (2012) 141–151, https://doi.org/10.4149/gpb_2012_015.
[5] A. Gyongyosi, et al., The role of autophagy and death pathways in Dose-dependent isoproterenolinduced cardiotoxicity, Curr. Pharm. Des. 25 (19) (2019) 2192–2198, https://doi.org/10.2174/1381612825666190619145025.
[6] R. Wang, Two’s company, three’s a crowd: can H2S be the third endogenous gaseous transmitter? FASEB J. 16 (13) (2002) 1792–1798, https://doi.org/10.1096/fj.02-0211hyp.
[7] R. Wang, Physiological implications of hydrogen sulfide: a whiff exploration that blossomed, Physiol. Rev. 92 (2) (2012) 791–896, https://doi.org/10.1152/physrev.00017.2011.
[8] S.J. Chan, P.T. Wong, Reprint of: hydrogen sulfide in stroke: protective or deleterious? Neurochem. Int 107 (2017) 78–87, https://doi.org/10.1016/j.neuint.2016.11.016.
[9] Y. Shen, et al., The cardioprotective effects of hydrogen sulfide in heart diseases: from molecular mechanisms to therapeutic potential, Oxid. Med. Cell Longev. 2015 (2015) 925167, https://doi.org/10.1155/2015/925167.
[10] A. Chhabra, et al., Glucose-6-phosphate dehydrogenase is critical for suppression of cardiac hypertrophy by H(2)S, Cell Death Discov. 4 (2018) 6, https://doi.org/10.1038/s41420-017-0010-9.
[11] J. Zhang, et al., Exogenous hydrogen sulfide supplement attenuates Isoproterenol-Induced myocardial hypertrophy in a sirtuin 3-dependent manner, Oxid. Med. Cell Longev. 2018 (2018) 9396089, https://doi.org/10.1155/2018/9396089.
[12] D. Chowdhury, et al., Prohibitin confers cytoprotection against ISO-induced hypertrophy in H9c2 cells via attenuation of oxidative stress and modulation of Akt/Gsk-3beta signaling, Mol. Cell Biochem. 425 (1-2) (2017) 155–168, https://doi.org/10.1007/s11010-016-2870-3.
[13] C.Y. Tsai, et al., E2/ER beta inhibit ISO-induced cardiac cellular hypertrophy by suppressing Ca2+-calcineurin signaling, PLoS One 12 (9) (2017) e0184153, https://doi.org/10.1371/journal.pone.0184153.
[14] W.B. Wei, et al., GYY4137, a novel hydrogen sulfide-releasing molecule, likely protects against high glucose-induced cytotoxicity by activation of the AMPK/mTOR signal pathway in H9c2 cells, Mol. Cell Biochem. 389 (1-2) (2014) 249–256, https://doi.org/10.1007/s11010-013-1946-6.
[15] M.M. Cerda, et al., Dithioesters: simple, tunable, cysteine-selective H(2)S donors, Chem. Sci. 10 (6) (2019) 1773–1779, https://doi.org/10.1039/c8sc04683b.
[16] P.M. Ridker, et al., A randomized trial of low-dose aspirin in the primary prevention of cardiovascular disease in women, N. Engl. J. Med. 352 (13) (2005) 1293–1304, https://doi.org/10.1056/NEJMoa050613.
[17] D.F. Caianiello, et al., Bifunctional small molecules that mediate the degradation of extracellular proteins, Nat. Chem. Biol. 17 (9) (2021) 947–953, https://doi.org/10.1038/s41589-021-00851-1.
[18] F. Liu, et al., STVNa attenuates Isoproterenol-Induced cardiac hypertrophy response through the HDAC4 and Prdx2/ROS/Trx1 pathways, Int. J. Mol. Sci. 21 (2) (2020), https://doi.org/10.3390/ijms21020682.
[19] K. Jeong, et al., Modulation of the caveolin-3 localization to caveolae and STAT3 to mitochondria by catecholamine-induced cardiac hypertrophy in H9c2 cardiomyoblasts, Exp. Mol. Med. 41 (4) (2009) 226–235, https://doi.org/10.3858/emm.2009.41.4.025.
[20] A. Gyongyosi, et al., BGP-15 protects against Doxorubicin-Induced cell toxicity via enhanced mitochondrial function, Int. J. Mol. Sci. 24 (6) (2023), https://doi.org/10.3390/ijms24065269.
[21] A. Gyongyosi, et al., Inhibited autophagy May contribute to heme toxicity in cardiomyoblast cells, Biochem. Biophys. Res. Commun. 511 (4) (2019) 732–738, https://doi.org/10.1016/j.bbrc.2019.02.140.
[22] A. Gurtler, et al., Stain-free technology as a normalization tool in Western blot analysis, Anal. Biochem 433 (2) (2013) 105–111, https://doi.org/10.1016/j.ab.2012.10.010.
[23] G. Corbi, et al., Adrenergic signaling and oxidative stress: a role for sirtuins? Front. Physiol. 4 (2013) 324, https://doi.org/10.3389/fphys.2013.00324.
[24] D. Yang, et al., Mitochondria in pathological cardiac hypertrophy research and therapy, Front. Cardiovasc. Med. 8 (2021) 822969, https://doi.org/10.3389/fcvm.2021.822969.

[25] E. Goldsborough, 3rd, et al., Assessment of cardiovascular disease risk: a 2022 update, Endocrinol. Metab. Clin. North Am. 51 (3) (2022) 483–509, https://doi.org/10.1016/j.ecl.2022.02.005.
[26] L. Zhang, et al., Hydrogen sulfide (H(2)S)-releasing compounds: therapeutic potential in cardiovascular diseases, Front. Pharm. 9 (2018) 1066, https://doi.org/10.3389/fphar.2018.01066.
[27] D. Kovacic, et al., Total plasma sulfide in congestive heart failure, J. Card. Fail 18 (7) (2012) 541–548, https://doi.org/10.1016/j.cardfail.2012.04.011.
[28] D. Chowdhury, et al., A proteomic view of isoproterenol induced cardiac hypertrophy: prohibitin identified as a potential biomarker in rats, J. Transl. Med. 11 (2013) 130, https://doi.org/10.1186/1479-5876-11-130.
[29] Z.W. Lee, et al., The slow-releasing hydrogen sulfide donor, GYY4137, exhibits novel anti-cancer effects in vitro and in vivo, PLoS One 6 (6) (2011) e21077, https://doi.org/10.1371/journal.pone.0021077.
[30] B. Geng, et al., Endogenous hydrogen sulfide regulation of myocardial injury induced by isoproterenol, Biochem. Biophys. Res. Commun. 318 (3) (2004) 756–763, https://doi.org/10.1016/j.bbrc.2004.04.094.
[31] K. Kondo, et al., H(2)S protects against pressure overload-induced heart failure via upregulation of endothelial nitric oxide synthase, Circulation 127 (10) (2013) 1116–1127, https://doi.org/10.1161/CIRCULATIONAHA.112.000855.
[32] A. Ahmad, et al., Up regulation of cystathione gamma lyase and hydrogen sulphide in the myocardium inhibits the progression of Isoproterenol-Caffeine induced left ventricular hypertrophy in wistar kyoto rats, PLoS One 11 (3) (2016) e0150137, https://doi.org/10.1371/journal.pone.0150137.
[33] G. Meng, et al., Hydrogen sulfide donor GYY4137 protects against myocardial fibrosis, Oxid. Med. Cell Longev. 2015 (2015) 691070, https://doi.org/10.1155/2015/691070.
[34] E. Dongo, et al., The cardioprotective potential of hydrogen sulfide in myocardial ischemia/reperfusion injury (review), Acta Physiol. Hung. 98 (4) (2011) 369–381, https://doi.org/10.1556/APhysiol.98.2011.4.1.
[35] A. Greasley, et al., H(2)S protects against cardiac cell hypertrophy through regulation of selenoproteins, Oxid. Med. Cell Longev. 2019 (2019) 6494306, https://doi.org/10.1155/2019/6494306.
[36] D.C. Andersson, et al., Mitochondrial production of reactive oxygen species contributes to the beta-adrenergic stimulation of mouse cardiomycytes, J. Physiol. 589 (Pt 7) (2011) 1791–1801, https://doi.org/10.1113/jphysiol.2010.202838.
[37] D.A. Brown, et al., Expert consensus document: mitochondrial function as a therapeutic target in heart failure, Nat. Rev. Cardiol. 14 (4) (2017) 238–250, https://doi.org/10.1038/nrcardio.2016.203.
[38] M.G. Rosca, C.L. Hoppel, Mitochondrial dysfunction in heart failure, Heart Fail Rev. 18 (5) (2013) 607–622, https://doi.org/10.1007/s10741-012-9340-0.
[39] M. Libiad, et al., Organization of the human mitochondrial hydrogen sulfide oxidation pathway, J. Biol. Chem. 289 (45) (2014) 30901–30910, https://doi.org/10.1074/jbc.M114.602664.
[40] V. Vitvitsky, et al., Cytochrome c reduction by H(2)S potentiates sulfide signaling, ACS Chem. Biol. 13 (8) (2018) 2300–2307, https://doi.org/10.1021/acschembio.8b00463.
[41] M. Shao, et al., Protective effect of hydrogen sulphide against myocardial hypertrophy in mice, Oncotarget 8 (14) (2017) 22344–22352, https://doi.org/10.18632/oncotarget.15765.
[42] O. Yamaguchi, Autophagy in the heart, Circ. J. 83 (4) (2019) 697–704, https://doi.org/10.1253/circj.CJ-18-1065.
[43] Y. Mei, et al., Autophagy and oxidative stress in cardiovascular diseases, Biochim. Biophys. Acta 1852 (2) (2015) 243–251, https://doi.org/10.1016/j.bbadis.2014.05.005.
[44] M. Bielawska, et al., Autophagy in heart failure: insights into mechanisms and therapeutic implications, J. Cardiovasc. Dev. Dis. 10 (8) (2023), https://doi.org/10.3390/jcdd10080352.
[45] R.Q. Dong, et al., Toll-like receptor 4 knockout protects against isoproterenol-induced cardiac fibrosis: the role of autophagy, J. Cardiovasc. Pharm. Ther. 20 (1) (2015) 84–92, https://doi.org/10.1177/1074248414539564.
[46] D. Wu, et al., Hydrogen sulfide and autophagy: a double edged sword, Pharmacol. Res. 131 (2018) 120–127, https://doi.org/10.1016/j.phrs.2018.03.002.
[47] C. Ott, et al., Hypertrophy-Reduced autophagy causes cardiac dysfunction by directly impacting cardiomyocyte contractility, Cells 10 (4) (2021), https://doi.org/10.3390/cells10040805.
[48] J. Wu, et al., Exogenous H(2)S facilitating ubiquitin aggregates clearance via autophagy attenuates type 2 diabetes-induced cardiomyopathy, Cell Death Dis. 8 (8) (2017) e2992, https://doi.org/10.1038/cddis.2017.380.
[49] L. Zhu, et al., Protective effect of hydrogen sulfide on endothelial cells through Sirt1-FoxO1-mediated autophagy, Ann. Transl. Med. 8 (23) (2020) 1586, https://doi.org/10.21037/atm-20-3647.